



PREPARATION AND CHARACTERIZATION OF SPINEL ZINC FERRITE $ZnFe_2O_4$

CHANDRASHEKHAR A. LADOLE*

Department of Chemistry, Sant Gadge Baba Amravati University, AMRAVATI – 444602 (M.S.) INDIA

ABSTRACT

Spinel zinc ferrite $ZnFe_2O_4$ was prepared by co-precipitation method using the ferric chloride $FeCl_3 \cdot 6H_2O$ and zinc chloride $ZnCl_2$ as raw materials and characterized by powder XRD, IR study and TG-DSC analysis. The influence of ferrite synthesis condition, such as Zn/Fe molar ratio, pH value and time was investigated. The results show that the pure spinel ferrite $ZnFe_2O_4$ are formed when the Zn/Fe molar ratio as 1 : 2 at pH = 7.5 and product was calcinated at 500°C for 5 hours.

Key words: Zinc ferrite, $ZnFe_2O_4$, Powder XRD, TG-DSC.

INTRODUCTION

At present, one of the most interesting and challenging issues of the science of magnetic nanoparticles is the introduction of new electronic, optical or photochemical properties and the optimization of their magnetic properties. Spinel zinc ferrite $ZnFe_2O_4$ has attracted more attentions due to its interesting magnetic property¹ and application in the catalysis²⁻⁵. Ferrite a ceramic like material with magnetic properties that are useful in many types of electronic devices. Zinc ferrite is a good example of the direct relation between the nanoparticle structure⁶, composition, and properties. When prepared as a bulk material, the zinc-iron oxide has a spinel structure AB_2O_4 with a tetrahedral A site occupied by Zn^{2+} ions and an octahedral B site by Fe^{3+} ions. Based on the distribution of cations, spinels can be either normal like zinc spinel or inverse with half of the trivalent ions in the tetrahedral position and the other half together with the divalent ions in the octahedral sites. Many types of methods including ceramic synthesis⁷, co-precipitation method⁸⁻¹⁰, tartrate precursor method¹¹, hydrothermal¹², combustion¹³, auto-combustion¹⁴, polymeric precursor route¹⁵, solvothermal¹⁶ and sol-gel technique¹⁷⁻¹⁸ etc. have been used to fabricate the precursor. Co-precipitation method has been intensively investigated to synthesized the precursor. For

* Author for correspondence; E-mail: ladoleshekhar2@gmail.com

example, spinel ZnFe_2O_4 could be synthesized at the 650°C for 6 h, which greatly reduce the production cost¹⁹.

Considerable interest has been attracted in current studies due to the large diversity and the practical usefulness of their physical and chemical properties, including humidity-sensing, oxygen-sensing, photoelectrical and super-paramagnetic as well as high temperature ceramic properties²⁰⁻²³. Therefore, it was thought of interest to synthesized zinc ferrite and it's characterization.

EXPERIMENTAL

All the chemicals and solvents were of analytical grade and purchased from commercial sources.

Zinc ferrite powder was prepared by two steps in first step the stoichiometric amount of zinc chloride (ZnCl_2) dissolved in distilled water and allowed to react with sodium hydroxide (NaOH) solution dissolved in distilled water with vigorous stirring and in second step a solution of ferric chloride $\text{FeCl}_3 \cdot 6\text{H}_2\text{O}$ prepared in HCl solution and mixed them and stirred for two hours and further heated for half an hour at 60°C . The mixture was allowed to settle and its pH adjusted to 7.5 with 2N sodium hydroxide solution (NaOH). The product obtained was washed by repeated decantation till free from chloride (Cl^-) ions and then filtered through a sintered glass crucible and then dried in oven at 120°C and then calcinated at 500°C for five hours. The product obtained was characterized by powder XRD, IR-spectroscopy and TG-DSC analysis.

Physical measurements

Power XRD measurement of the Ferrite was recorded with a Bruker AXS-D8 Advanced model X-ray diffractometer with $\text{Cu K}\alpha$ 1.5 line ($\lambda = 1.54056 \text{ \AA}$) in 2θ range from 10° - 90° . IR spectra were recorded as KBr pellets on a Perkin-Elmer-1600 FT-IR spectrophotometer. TG-DSC analyses of ferrite were carried out using a SETARAM instrument, Model 92-16.18, on the part of dried gel precursors in the flowing air atmosphere with the heating rate of $10^\circ\text{C}/\text{min}$.

RESULTS AND DISCUSSION

Powder XRD analysis

A typical XRD pattern of the synthesized ZnFe_2O_4 nanocrystal as shown in Fig. 1. The ZnFe_2O_4 nanoparticles have a degree of crystallinity. The XRD pattern of zinc ferrite

prepared by co-precipitation method was match of with those reported by others conforming the cubic structure and formation of tetragonal form is ruled out. The particle size was calculated using Scherer formula. The particle size was found to vary in the range 37.58-57.52 nm.

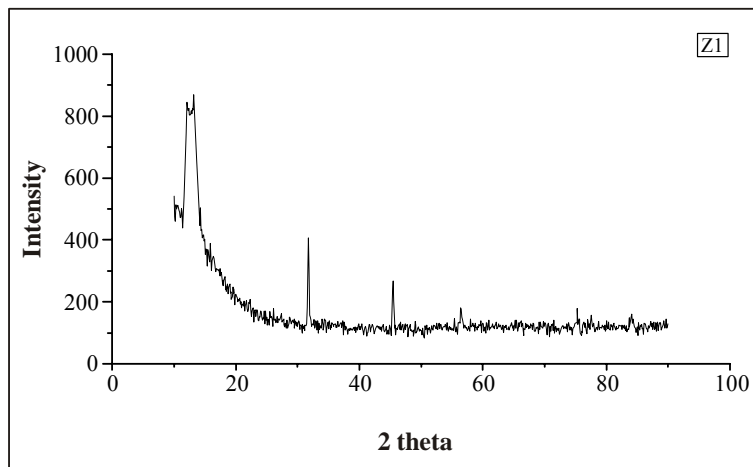


Fig. 1: XRD pattern of ZnFe₂O₄

FT-IR Analysis

The IR spectrum of the precursor material, when taken from the oven, shows the typical bands of the support associated to the skeleton of the spinel. It can be observed the most intense band of the spectrum, splitted in 1355 cm^{-1} and 880 cm^{-1} , due to the stretching of Zn-O-Fe bonds of the tetrahedral building units forming the structure. The wide absorption in the high energy region of the spectrum, centered at 3501 cm^{-1} , resulting from -OH stretching, is associated to the vibration of water molecules coordinated to ferrite structure. In addition, the HOH deformation mode of the same bonds is placed in 1632 cm^{-1} . It is worth mentioning that in catalysts supported on ferrite, these bands are overlapped with the vibrations belonging to the same species presents in the precursor when it is taken from the oven. The broadening of the 3451 cm^{-1} band towards lower frequencies may be due to the formation of H bridges in the precursor, which subsequently disappear with the thermal treatment.

After the thermal treatment at 150°C the main absorption attributed to the complex have disappeared and only one weak band is observed at 1465 cm^{-1} indicating the complete thermal degradation of the precursor. The IR spectra of the samples do not show significant changes in the thermal range between $400\text{-}700^{\circ}\text{C}$, except for the modifications that are observed in the stretching band -OH, in the high energy region of the spectra.

TG-DSC Analysis

TG-DSC Analysis of zinc ferrite was done. In TG-DSC analysis of ferrite shows Fe, Zn and O elements identified. During heating chemical change of zinc ferrite is take place. From the DSC curve two endothermic peaks appear near 76°C and 130°C which are caused due to desorption of water²⁴. While rapid decrease of TG-curve with a weight loss of 8-10% is observed. One exothermic peak between 160°C and 570°C is observed with weight loss of 19.12% which is caused by decomposition of Fe and Zn hydroxides. Also one tiny exothermic peak appearing near 870°C almost without any weight loss this due to formation of zinc oxide²⁵.

CONCLUSION

The spinel ferrite can be obtained by co-precipitation method using zinc chloride and ferric chloride as a raw materials. The result shows that the spinel zinc ferrite $ZnFe_2O_4$ are formed when molar ratio Zn/Fe is 1 : 2 at pH = 7.5 and the product obtained by calcinateing at 500°C for five hours which greatly reduce the production cost.

ACKNOWLEDGMENT

The author is thankful to Sant Gadge Baba Amravati University, Amravati for providing research facilities and encouragement.

REFERENCES

1. C. Yao, Q. Zeng, G. F. Goya, T. Torres, J. Liu, H. Wu, M. Ge and J. Z. Jiang, J. Phys. Chem., **111**, 12274 (2007).
2. Y. Chung, Y. Kwon, T. Kim, S. Lee and S. Hoon, Catal. Lett., **131**, 579 (2009).
3. J. Wolska, K. Przepiera, H. Grabowska, A. Przepiera, M. Jablonski and R. Klimkiewicz, Res. Chem. Intermed., **34(1)**, 43 (2008).
4. R. Klimkiewicz, J. Wolska, A. Przepiera, K. Przepiera, M. Jablonski and S. Lenart, Mater. Res. Bull., **44**, 15 (2009).
5. H. Lee, J. Jung, H. Kim, Y. Chung, T. Kim, S. Lee, S. Oh, Y. Kim and I. K. Song, Catal. Lett., **122**, 281 (2008).
6. Y. Li, R. Yi, A. Yan, L. Deng, K. Zhou and X. Liu, Solid State Sci., **11**, 1319 (2009).
7. C. N. Chinnasamy, A. Narayanasamy and N. Ponpandian, J. Phy. Cond. Matter., **12**, 7795 (2000).

8. D. Makovec, A. Kodre, I. Arcon and M. Drogenik, *J. Nanopart Res.*, **13**, 1781 (2011).
9. D. Makovec, A. Kodre, I. Arcon and M. Drogenik, *J. Nanopart Res.*, **11**, 1145 (2009).
10. M. Maletin, E. G. Moshopoulou, A. G. Kontos, E. Devlin, A. Delimitis, V. T. Zaspalis, L. Nalbandian and V. V. Srdic, *J. Eur. Ceram. Soc.*, **27**, 4391 (2007).
11. J. M. Yang and K. L. Yang, *J. Nanopart Res.*, **11**, 1739 (2009).
12. L. Nalbandian, A. V. Delimitis, T. Zaspalis, E. A. Deliyanni, D. N. Bakoyannakis and E. N. Peleka, *Microporous Mesoporous Mater.*, **114**, 465 (2008).
13. M. Sertkol, Y. Koseoglu, A. Baykal, H. Kavas and M. S. Toprak, *J. Magn. Magn. Mater.*, **322**, 866 (2010).
14. M. R. Barati, S. A. S. Ebrahimi and A. Badiei, *J. Non-Cryst. Solids*, **354**, 5184 (2008).
15. M. Gharagozlu, *J. Alloys Compd.*, **486**, 660 (2009).
16. S. Yanez-Vilar, M. Sanchez-Andujar, C. Gomez-Aguirre, J. Mira, M. A. Senaris-Rodriguez and S. Castro-Garcia, *J. Solid State Chem.*, **182**, 2685 (2009).
17. G. Aurelija, J. Darius, B. Aldona and K. Aivaras, *Mater. Sci.*, **17(3)**, 302 (2011).
18. B. Zhang, J. Zhang and F. Chen, *Res. Chem. Intermed.*, **34(4)**, 375 (2008).
19. H. Lee, J. C. Jung and H. Kim, *Catal. Commun.*, **9**, 1137 (2008).
20. W. F. J. Fontijn, P. J. Van der Zaag, L. F. Feiner, R. Metselaar and M. A. C. Devillers, *J. Appl. Phys.*, **85**, 5100 (1999).
21. W. Schafer, W. Kockelman, A. Kirfel, W. Potzel, F. J. Burghart, G. M. Kalvius, A. Martin, W. A. Kaczmarek and S. J. Campbell, *Mater. Sci. Forum*, **321**, 802 (2000).
22. H. H. Hamdeh, J. C. Ho, S. A. Oliver, R. J. Willey, G. Oliveri and G. Busca, *J. Appl. Phys.*, **81**, 1851 (1997).
23. S. A. Oliver and H. H. Hamdeh, *Phys. Rev.*, **B 60**, 3400 (1999).
24. J. C. Yu, J. G. Yu, W. K. Ho, Z. T. Jiang and L. Z. Zhang, *Chem. Mater.*, **14**, 3808 (2002).
25. R. Arulmurugan, G. Vaidyanathan, S. Sendhilnathan and B. Jeyadevan, *J. Magn. Magn. Mater.*, **298**, 83 (2006).

Accepted : 13.06.2012